



OPEN

An appraisal of lung computer tomography in very early anti-inflammatory treatment of two different ovine ARDS phenotypes

Karin Wildi^{1,2,3,10}✉, Sebastiano Maria Colombo^{1,2,4,10}, Daniel McGuire^{1,2,5}, Carmen Ainola^{1,2}, Silver Heinsar^{1,2,6}, Noriko Sato¹, Kei Sato^{1,2}, Keibun Liu¹, Mahé Bouquet², Emily Wilson², Margaret Passmore^{1,2}, Kieran Hyslop^{1,2}, Samantha Livingstone^{1,2}, Marianna Di Feliciano⁴, Wendy Strugnell^{2,5}, Chiara Palmieri⁷, Jacky Suen^{1,2}, Gianluigi Li Bassi^{1,2,8,9}✉ & John Fraser^{1,2,8}

Mortality and morbidity of Acute Respiratory Distress Syndrome (ARDS) are largely unaltered. A possible new approach to treatment of ARDS is offered by the discovery of inflammatory subphenotypes. In an ovine model of ARDS phenotypes, matching key features of the human subphenotypes, we provide an imaging characterization using computer tomography (CT). Nine animals were randomized into (a) OA (oleic acid, hypoinflammatory; n = 5) and (b) OA-LPS (oleic acid and lipopolysaccharides, hyperinflammatory; n = 4). 48 h after ARDS induction and anti-inflammatory treatment, CT scans were performed at high (H) and then low (L) airway pressure. After CT, the animals were euthanized and lung tissue was collected. OA-LPS showed a higher air fraction and OA a higher tissue fraction, resulting in more normally aerated lungs in OA-LPS in contrast to more non-aerated lung in OA. The change in lung and air volume between H and L was more accentuated in OA-LPS, indicating a higher recruitment potential. Strain was higher in OA, indicating a higher level of lung damage, while the amount of lung edema and histological lung injury were largely comparable. Anti-inflammatory treatment might be beneficial in terms of overall ventilated lung portion and recruitment potential, especially in the OA-LPS group.

Abbreviations

ARDS	Acute respiratory distress syndrome
ATS	American thoracic society
CT	Computer tomography
EELV	End-expiratory lung volume
ELISA	Enzyme-linked immunoassay
FiO ₂	Inspired oxygen fraction
H	CT scan performed with high airway pressure
HU	Hounsfield unit
HR	Heart rate

¹Critical Care Research Group, The Prince Charles Hospital, Rode Road, Chermside, Brisbane, QLD 4032, Australia. ²The University of Queensland, Brisbane, Australia. ³Cardiovascular Research Institute Basel, University Hospital Basel, University of Basel, Basel, Switzerland. ⁴Department of Anaesthesia and Intensive Care Medicine, Fondazione IRCCS Ca' Granda Ospedale Maggiore Policlinico, Milan, Italy. ⁵The Prince Charles Hospital, Chermside, QLD, Australia. ⁶Department of Intensive Care, North Estonia Medical Centre, Tallinn, Estonia. ⁷School of Veterinary Science, The University of Queensland, Gatton, Australia. ⁸St Andrews War Memorial Hospital, Intensive Care Unit, Spring Hill, QLD, Australia. ⁹The Wesley Hospital, Intensive Care Unit, Auchenflower, QLD, Australia. ¹⁰These authors contributed equally: Karin Wildi and Sebastiano Maria Colombo. ✉email: wildik@hotmail.com; gianluigilibassi@gmail.com

IL	Interleukin
IQR	Interquartile range
IV	Intravenously
L	CT scan performed with low airway pressure
LIS	Lung injury score
LPS	Lipopolysaccharide
MAP	Mean arterial pressure
mPAP	Mean pulmonary artery pressure
NF- κ B	Nuclear factor-kappa B pathway
NS	Normal saline
OA	Oleic acid
OA-ctr	OA control
OA-pred	OA treated with methylprednisolone
OA-ery	OA treated with erythromycin
OA-LPS	Oleic acid and lipopolysaccharides
OA-LPS-ctr	OA-LPS control
OA-LPS-pred	OA-LPS treated with methylprednisolone
OA-LPS-ery	OA-LPS treated with erythromycin
Pdriv	Driving pressure
PF ratio	PaO ₂ /FiO ₂ ratio
PEEP	Positive end-expiratory pressure
QUT	Queensland University of technology
RM	Recruitment maneuver
SD	Standard deviation
VILI	Ventilation-induced lung injury

Since the first description of ARDS in 1967¹, numerous different research approaches have been trialed for better characterization and understanding of the pathophysiology of the syndrome, aimed to define treatable traits that will ultimately allow a better outcome for patients. Imaging studies have been instrumental in understanding regional lung inhomogeneities in ARDS² and deleterious effects of mechanical ventilation^{3,4}, namely ventilation-induced lung injury (VILI)⁵. Consecutively, the recruitment potential of ARDS lungs was assessed with imaging techniques to further understand pathophysiological underpinnings leading to lung damage^{6–8}. A landmark study was published in 2006⁹, quantifying the recruitment potential in ARDS and associating high recruitment potential with worse survival rates. Furthermore, the nowadays well-established concept of prone positioning in severe ARDS^{10–12} was studied in translational models using imaging technology^{13–15}.

Irrespective of abovementioned findings, ARDS morbidity and mortality remain largely unchanged¹⁶. A recent discovery might offer an explanation: the heterogeneous population of ARDS patients seems to consist of two subgroups, a hyperinflammatory and a hypoinflammatory subphenotype^{17–21}. Post-hoc analyses of clinical trials in ARDS emphasized potentially overlooked benefits of treatments when applied to the hyperinflammatory subphenotype alone^{22–24}. Enrichment strategies in general²⁵ and in ARDS specifically²⁶ will likely guide future studies and therapies towards personalized therapy²⁷.

Such enrichment approaches have been tried using imaging technology in ARDS: by differentiating pulmonary and extrapulmonary causes of ARDS²⁸ and describing the distribution of aerated lung compartments²⁹, Wendel et al. assessed pulmonary phenotypes with imaging and reported 2 subgroups: phenotype 1 was designated by lower lung inhomogeneities, dead space ventilation, and elastance; whereas the hallmarks of phenotype 2 were a higher compliance and recruitment potential but also higher mortality. The study suggests that phenotype 2 might provide at least some overlap with the hyperinflammatory subphenotype, as lower compliance and a higher amount of acidosis have been reported in both. In a recent intervention study³⁰ patients were randomized to a personalized ventilation strategy according to their imaging phenotype—focal or non-focal ARDS—but no survival benefit could be demonstrated.

Imaging will be essential to enhance our understanding of the pathophysiology and morphology of ARDS subphenotypes. Therefore, our group developed³¹ and validated³² large animal models of ARDS phenotypes, demonstrating that the double-hit model using oleic acid (OA) and lipopolysaccharides (LPS) shares some essential features with the human hyperinflammatory subphenotype. OA alone was pragmatically chosen as the opposite lung injury model with the least systemic inflammation response as compared to OA-LPS. In an intervention study, animals were then treated with anti-inflammatory agents (methylprednisolone or erythromycin) and monitored for up to 48 h. The hyperinflammatory lung injury model treated with methylprednisolone alone was shown an early and consistent improvement in oxygenation³³. This subanalysis aimed to describe pulmonary volumes (air and tissue) and aeration states in ovine ARDS phenotypes treated with anti-inflammatory agents to test the hypothesis that hyperinflammatory ovine ARDS might benefit from treatment in terms of recruitment potential.

Materials and methods

Animal studies were conducted at the Queensland University of Technology (QUT) Medical Engineering Facility (MERF) in Brisbane, Australia. The study was assessed and approved by the QUT Office of Research Ethics and Integrity (No 18-606). All experiments were performed in accordance with the Australian Code of Practice for the Care and Use of Animals for Scientific Purposes and the Animal care and Protection Act 2001 (QLD) and complied with the ARRIVE Guidelines³⁴.

Study design

This study was an additional experiment of a study designed to assess the efficacy of anti-inflammatory treatment in two models of ARDS injury in an ovine model (Supplementary Figure S1A)³³. A lung CT scan was performed in all animals that survived until study end at 48 h if the scanner was available.

Animal preparation and intra-experimental monitoring/management

All animals were instrumented with a jugular central venous line (CVL) and sheath for Swan Ganz catheter. General anesthesia was induced by using midazolam and propofol intravenously, then the animal was endotracheally intubated. Further instrumentation consisted of femoral arterial line, nasogastric tube, urinary catheter and bilateral pleural drains. Additionally, a surgical tracheostomy was performed in all animals. Lung-protective ventilation was applied as according to the EXPRESS trial³⁵. After completing all instrumentation steps, the animal rested for 1 h, then ARDS was induced. Intra-experimental monitoring, management and data collection has been reported in detail before^{31,33}.

ARDS induction and anti-inflammatory treatment

Randomization was performed using a random number generator. Animals randomized to OA received sequential doses of oleic acid (OA, 0.89 g/ml at 25 °C; 01008, Sigma-Aldrich, Australia) intravenously (IV) in subsequent doses of 0.03 ml/kg until a PaO₂/FiO₂ ratio (PF) of < 150 mmHg was achieved (= ARDS diagnosis, T0) as assessed by arterial blood gas analysis every 15 min. OA-LPS animals received OA as reported above, after reaching the PF goal, 0.5 µg/kg of lipopolysaccharide (LPS: E. coli O55:B5, Sigma-Aldrich, Australia), dissolved in 50 ml of normal saline was given IV over 1 h.

In animals randomized to treatment with methylprednisolone, 100 mg as a bolus was applied IV at T0, afterwards 2 mg/kg/24 h was administered as a continuous infusion. Erythromycin was applied as 100 mg bolus IV every 6 h after T0. As investigators conducting the clinical experiments were blinded to study treatment, every animal received two boluses of 10 ml at T0 (one containing methylprednisolone 100 mg or normal saline (NS) and one containing erythromycin 100 mg or NS) and a consecutive infusion of 2 ml/h (containing methylprednisolone 2 mg/kg/24 h or NS) as well as a bolus of 10 ml every 6 h (containing erythromycin 100 mg or NS).

Outcomes

In animals with OA and OA-LPS lung injury, we compared lung volumes and recruitable lung tissue between animals that were treated with anti-inflammatory agents.

Lung computer tomography at T48h

A Toshiba Acquilion Lightning Computed Tomography Scanner (Canon Medical Care, Japan) was used in this study. Scanner settings were set as previously validated⁹: Acquisition 16 × 1 mm reconstructed to slice thickness 5 mm, interval 5 mm, bed speed 15 mm per second, voltage 135 kV and current non-modulated 240 mA. The sequence of the CT study is shown in Supplementary Figure S1B. Scans were taken at 5 and 45 (arbitrarily defined as total lung capacity) cmH₂O of airway pressure.

All scans were performed in prone position utilizing consistent scan ranges. First, after administration of 10 mg of vecuronium, pressure-controlled ventilatory mode was used for a recruitment maneuver (RM) set to an inspiratory plateau pressure of 45 cm H₂O and a PEEP of 15 cm H₂O (inspiration to expiration ratio (I:E) 1:1, FiO₂ 100%, respiratory rate 10 per minute). The maneuver was terminated after 10 breaths and after setting the peak inspiratory pressure to 45 cm H₂O, the endotracheal tube was clamped during an inspiratory pause and the first whole lung scan performed (high airway pressure: H). After the H scan, the animal was allowed to rest for 10 min, using volume-controlled ventilatory settings as before the RM for respiratory rate, tidal volume and I:E. FiO₂ left at 100% and PEEP decreased to 5cmH₂O. After completion of the resting period, the endotracheal tube was clamped during expiratory pause and the second whole lung scan was performed (low airway pressure: L).

Analysis of cross-sectional lung images

Post-acquisition CT scan analysis was performed with a dedicated software (Maluna 3.17, University Hospital of Göttingen, Göttingen, Germany). Lung CT images were manually outlined including only lung parenchyma and excluding bronchi and large intrapulmonary vessels to measure lung gas content, lung weight and aeration distribution. Further details about CT scan analysis have been provided elsewhere^{36–38}. The CT numbers are expressed as Hounsfield Units (HU) which reflect the density of the tissue (volume of gas/volume of tissue), resulting in an estimation of the weight of lung compartments⁶. The distribution of aeration compartments was then assessed as fractions of lung weight and categorized according to HU (gas/tissue content) as not aerated (CT number between + 100 and -100 HU, poorly aerated (CT number between -101 and -500 HU), normally aerated (-501 and -900 HU) and over-aerated (-901 and -1,000 HU). Each slice was then divided into 10 horizontal segments to obtain the ventro-dorsal gradient of density distribution from non-dependent (number 1) to dependent (number 10) to lung regions. Lung tissue weight of each compartment was expressed as a percentage of the total lung weight. We defined recruitment as the variation from non-aerated / poorly aerated region to normally aerated when comparing L and H scans. Dynamic strain was calculated as tidal volume divided by end-expiratory lung volume (EELV, as gas volume at low pressure)^{3,39}.

Measurement of inflammatory cytokines

Arterial blood samples were collected in EDTA blood tubes and processed to plasma, samples were then stored at - 80 °C until batch analysis. Plasma concentration of inflammatory cytokines (e.g. interleukin (IL) -6, -8, -10)

were quantified by in-house ELISAs⁴⁰. Positive internal controls were used to ensure that inter- and intra-plate variability was < 10% and to confirm the precision of all the assays.

Histopathology assessment

Animals were euthanized after the CT scan and lung tissue was taken for histological assessment. Lung tissue was preserved in 10% neutral buffered formalin for 24 h, then embedded in paraffin, sectioned to a 5 µm thickness and stained with hematoxylin&eosin using standard procedures. Slides were examined by an independent, blinded, qualified veterinary pathologist and lung injury score was assessed as recommended by the ATS for experimental ARDS in animal models⁴¹ (Supplemental Methods and Supplementary Table S1 Online Suppl.). Pulmonary edema was quantified by the wet-to-dry-weight of post-mortem left and right upper and lower lung lobe.

Statistical analysis

Categorical variables are reported as numbers and percentages and continuous data as mean ± standard deviation (SD). Comparisons between groups were made using Kruskal–Wallis test or Mann–Whitney U test as appropriate. Paired continuous parameters were assessed by a paired sample t-test, while categorical were analyzed by Friedmans 2-way analysis of variance for ranks. All hypothesis testing is two-tailed and p-value of less than 0.05 was considered statistically significant. All statistical analyses were performed with SPSS for Mac 27.0 (SPSS Inc, Chicago, USA).

Results

Studied population

Nine female non-pregnant Merino-Dorset crossbreed ewes, aged 1–3 years, with a mean weight of 53 (± 5) kg, were eligible for this analysis. 5 animals were randomized to OA (4 treated with methylprednisolone and 1 treated with erythromycin) and 4 animals to OA-LPS (3 treated with methylprednisolone and 1 with erythromycin) (Supplementary Figure S1A). Baseline characteristics among the two injury models showed no differences (Supplementary Table S2).

Lung volumes in OA and OA-LPS phenotypes

Overall, OA animals showed substantially more non-aerated and poorly aerated lung tissue than OA-LPS, whereas OA-LPS displayed a higher amount of normally aerated lung tissue than OA ($p < 0.05$). The fraction of overinflated lung was low in OA and OA-LPS (Fig. 1, Supplementary Figure S3).

Total lung volume in OA was 2510 ml (IQR 1778–3657 ml) during H and 2338 ml (IQR 2026–2960 ml) during L, the respective volumes in OA-LPS were 2993 ml (IQR 2634–4043 ml) and 2759 ml (IQR 2249–2696 ml) (Fig. 2). All total lung volumes followed a similar dorso-ventral distribution in OA and OA-LPS, with the highest volumes in slices 2 to 8 (non-dependent to dependent). Distribution of all assessed volumes (total lung volume, air, tissue and gas-tissue ratio) in H and L and in OA and OA-LPS separately, were not the same among slices dorsal to ventral (all $p < 0.05$) (Fig. 2). The total lung volume was comparable among OA and OA-LPS, whereas there

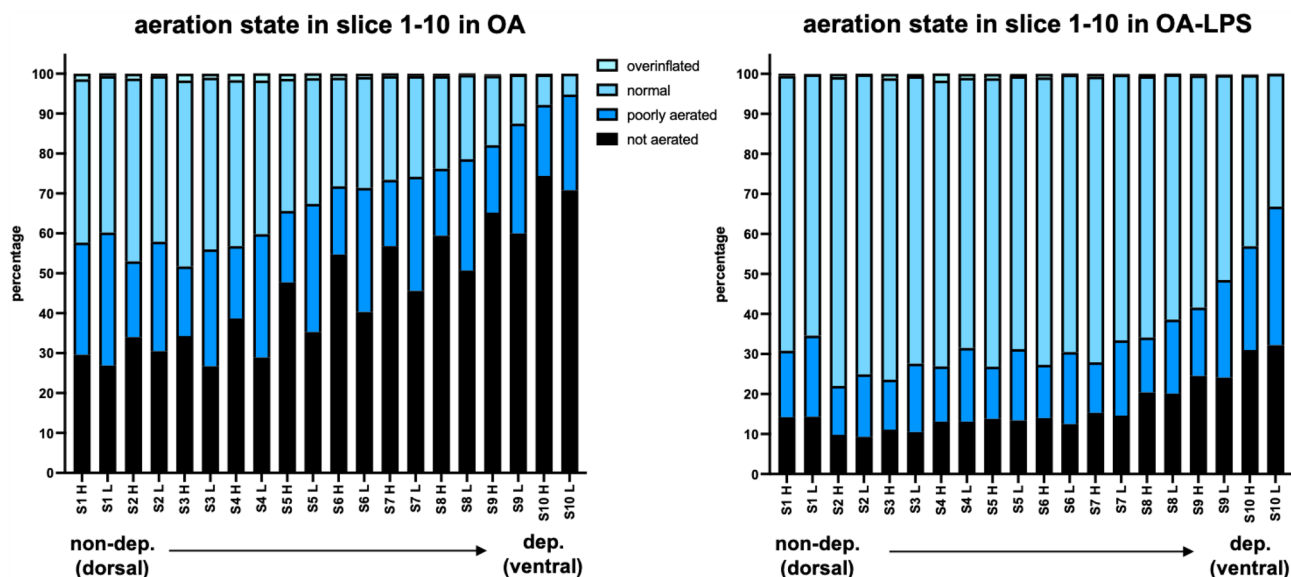


Figure 1. Aeration states in dorso-ventral distribution between high and low airway pressure scans among ARDS phenotypes. H, CT scan performed with high airway pressure; L, CT scan performed with low airway pressure; OA, oleic acid; OA-LPS, oleic acid and lipopolysaccharides. Comparison of the 4 aeration states over slice 1 to 10 for H and L in OA and OA-LPS: OA, (a) overinflated L and H $p < 0.001$, (b) normal L and H, not aerated H $p < 0.01$, (c) not aerated L $p < 0.05$. OA-LPS, (a) overinflated L and H, normal L and H, not aerated L and H $p < 0.01$, (b) overinflated L $p < 0.05$.

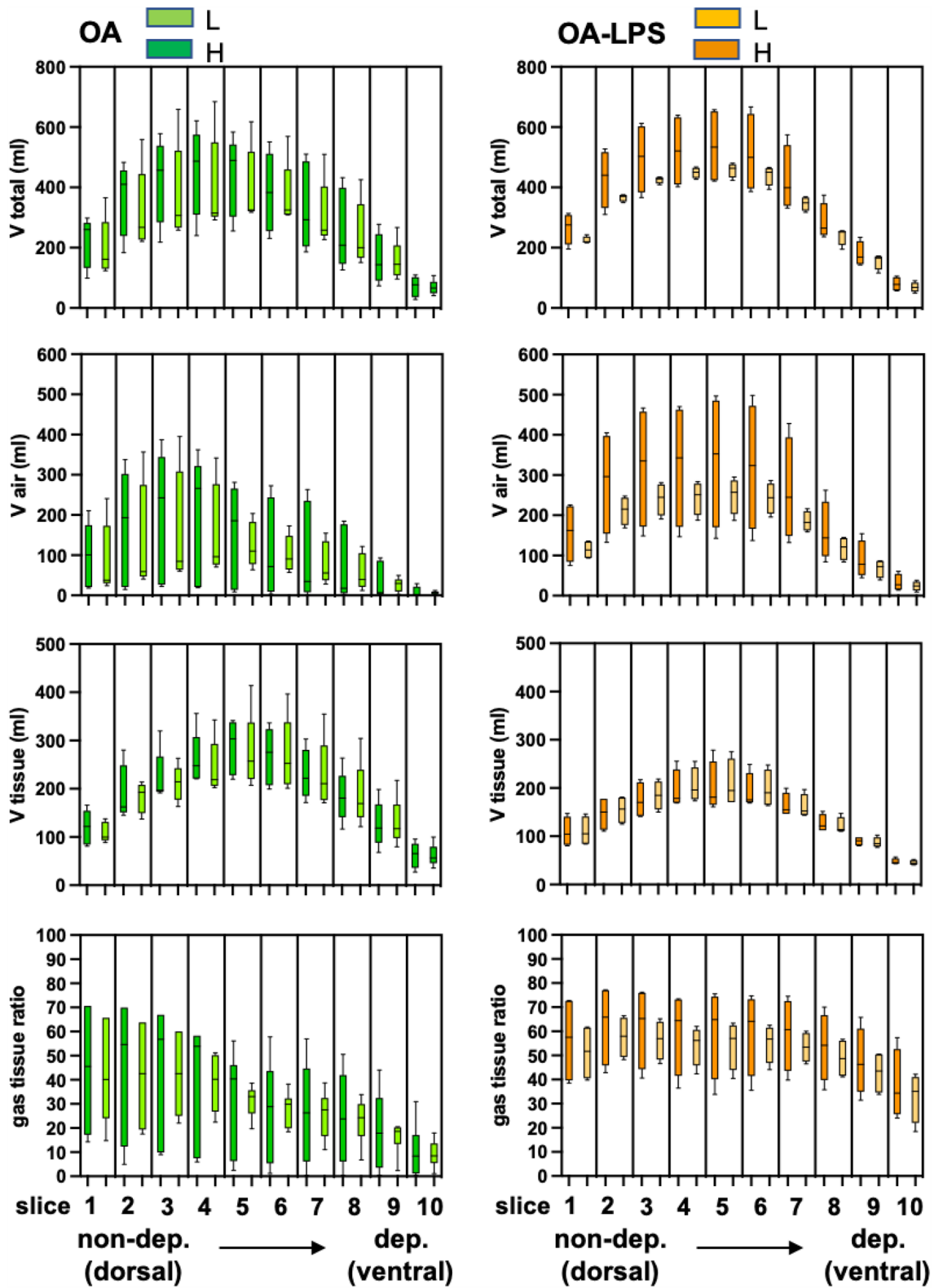


Figure 2. Changes in lung volumes between high and low airway pressure scans among the two ARDS injury types. V, volume; ml, milliliter; H, CT scan performed with high airway pressure; L, CT scan performed with low airway pressure; OA, oleic acid; OA-LPS, oleic acid and lipopolysaccharides.

was a trend towards higher air fraction in OA-LPS and higher tissue fraction in OA in the non-dependent slices (Fig. 2). Strain was higher in OA (0.45, IQR 0.25–0.74) than in OA-LPS (0.18, IQR 0.16–0.23; p 0.05) (Fig. 3).

Changes in lung volumes according to low and high airway pressure among OA and OA-LPS

The change in total lung volume and air volume between high (H) and low airway pressure (L) per each slice was more accentuated in OA-LPS than OA (p for trend < 0.05), reflecting a higher recruitment potential, whereas the change in tissue volume was comparable among OA and OA-LPS. The change in gas-tissue ratio between L and H was comparable among OA and OA-LPS, but OA-LPS displayed a higher ratio over all slices (Fig. 2; Supplementary Figure S2).

In OA and OA-LPS, there was a higher proportion of normally aerated lung and a lower fraction of poorly aerated lung in H as compared to L (comparison of the 4 aeration states over slice 1 to 10 (non-dependent to dependent) for H and L: $p < 0.05$). Only in OA animals, the fraction of non-aerated lung was higher in H as compared to L while in OA-LPS it remained largely similar among H and L.

Clinical and laboratory assessment of animals at 48 h (before CT scan)

Up to 24 h, OA-LPS animals required more vasopressor support, whereas at 48 h (just before the CT scan), they were shown a higher SVRI and lower heart rate with less vasoactive support than OA animals (Table 1). While compliance and EVLWI were comparable among the injury models, driving pressure and dead space ventilation were lower in OA-LPS animals throughout the study. PF ratio remained consistently higher and oxygenation index lower in OA-LPS as compared to OA animals. OA-LPS displayed higher lymphocyte and neutrophil counts than OA (Table 1).

Histopathology assessment

The mean LIS was $0.44 (\pm 0.09)$ for OA and $0.40 (\pm 0.08)$ for OA-LPS ($p = ns$). Necrosis score was $0.54 (\pm 0.3)$ in OA and $0.05 (\pm 0.1)$ in OA-LPS ($p 0.016$) (Fig. 4A). More bacterial colonies were found in OA (3/5 animals) than in OA-LPS (0 animals), and the presence of alveolar hemorrhage was described in 3/5 animals in OA and 1/4 in OA-LPS (Fig. 4B). Wet-dry ratio was comparable among OA (mean 9.5 ± 2.2) and OA-LPS (mean 7.7 ± 0.9) ($p = ns$).

Levels of inflammatory cytokines

Levels of IL-6 were significantly higher in OA-LPS at 12 and 24 h as compared to OA, but assimilating towards study end. Levels of IL-8 and IL-10 were slightly higher in OA than OA-LPS animals throughout the observation period (Table 1).

Discussion

This is an innovative preclinical imaging study of 2 different ovine ARDS phenotypes treated with anti-inflammatory agents. This study represents the first animal report assessing CT characterization of different ARDS phenotypes, reporting on six clinically relevant findings.

First, the highest lung volumes were seen in non-dependent lung areas in both injury types, following a gravitational distribution. *Second*, the total lung volume was comparable among lung injury types, while there was a higher air fraction in OA-LPS and a higher tissue fraction in OA. Thus, there was an increased fraction of normally aerated lungs in OA-LPS in contrast to a higher fraction of non-aerated lung in OA. *Third*, the change in lung and air volume between H and L was more accentuated in OA-LPS than OA, indicating a higher recruitment potential. In contrast, the change in tissue volume from H to L was comparable among OA and OA-LPS. *Fourth*, in response to recruitment maneuvers, both phenotypes showed more normally aerated and less poorly aerated lung in H as compared to L. However, in OA alone, the fraction of non-aerated lung increased at H when compared to L while it remained similar in OA-LPS. *Fifth*, strain was higher in OA, indicating a higher level of lung

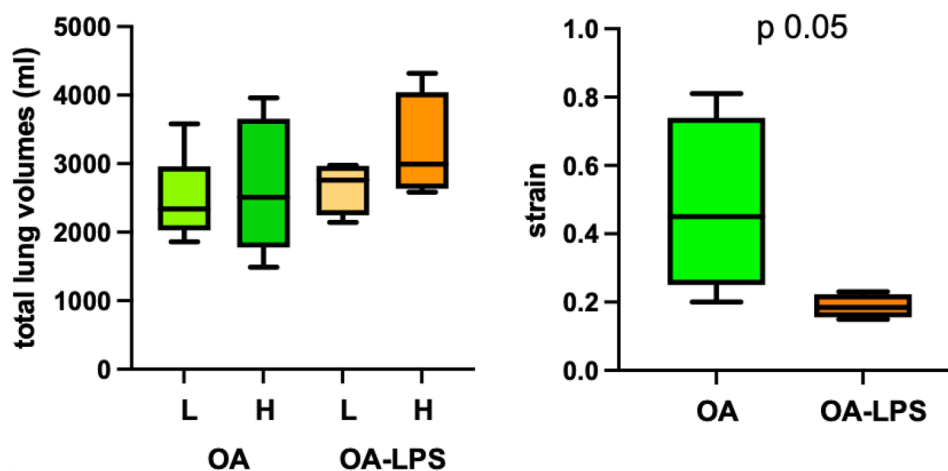


Figure 3. Total lung volumes and strain among different ARDS injury types. H, CT scan performed with high airway pressure; L, CT scan performed with low airway pressure; OA, oleic acid; OA-LPS, oleic acid and lipopolysaccharides.

	at 12 h		at 24 h		at 48 h	
	OA (n=5)	OA-LPS (n=4)	OA (n=5)	OA-LPS (n=4)	OA (n=5)	OA-LPS (n=4)
Hemodynamic parameters						
Mean arterial blood pressure (mmHg)	73 (9)	77 (15)	75 (11)	79 (7)	70 (10)	76 (9)
Heart rate (bpm)	73 (18)	97 (15)	96 (19)	82 (7)	95 (30)	66 (7)
Mean pulmonary artery pressure (mmHg)	22 (5)	18 (4)	26 (7)	20 (2)	20 (3)	17 (2)
Cardiac index (L/min/m ⁰)	3.4 (1.1)	3.6 (0.4)	4.7 (0.7)	4.3 (0.7)	5.3 (1.6)	4.0 (0.8)
Systemic vascular resistance index (meana dyn*s*cm ⁻⁵ *m ²)	1910 (565)	1609 (64)	1252 (337)	1676 (487)	1120 (394)	1484 (262)
Dose of noradrenaline (mcg/kg/min)	0.04 (0.05)	0.15 (0.09)	0.05 (0.07)	0.11 (0.08)	0.15 (0.14)	0.04 (0.05)
Mechanical ventilation						
Minute ventilation (L/min)	8.7 (2.5)	9.8 (1.6)	9.7 (4.6)	9.5 (2.2)	12.1 (3.0)	9.9 (3.7)
Compliance (mL/cmH ₂ O)	21 (4)	21 (5)	21 (5)	22 (6)	20 (3)	22 (4)
PEEP (cmH ₂ O)	9 (1)	8 (0)	8 (1)	8 (0)	7 (1)	8 (1)
Driving pressure (cm H ₂ O)	15 (4)	13 (3)	17 (8)	12 (5)	16 (2)	13 (3)
Extravascular lung water index	40 (12)	48 (6)	43 (13)	41 (7)	45 (2)	42 (6)
Oxygenation index	12 (8)	9 (4)	29 (18)	9 (6)	24 (19)	11 (6)
Dead space ventilation (in ml)	60 (89)	26 (44)	57 (122)	19 (33)	135 (91)	46 (62)
Shunt (%)	29 (14)	22 (6)	18 (5)	25 (5)	15 (4)	24 (7)
Blood gases						
PaO ₂ /FiO ₂ ratio	243 (109)	259 (88)	169 (92)	263 (97)	149 (95)	213 (80)
PaCO ₂ (mmHg)	43 (3)	48 (4)	52 (3)	42 (4)	47 (12)	47 (7)
Lactate	2.0 (0.8)	3.1 (0.9)	2.1 (1.8)	2.6 (0.4)	1.9 (0.3)	1.4 (0.5)
Base excess (mmol/L)	1.8 (4.3)	-1.1 (0.8)	-0.2 (6.3)	-1.7 (1.4)	0.4 (2.2)	2.0 (1.8)
Full blood count						
Hemoglobin (g/L)	109 (16)	127 (24)	109 (11)	110 (12)	103 (6)	102 (13)
Platelets (×10 ⁹ /L)	197 (97)	226 (73)	201 (71)	189 (52)	153 (51)	189 (26)
Neutrophil count (×10 ⁹ /L)	3.0 (2.0)	3.6 (1.5)	2.6 (2.8)	4.8 (2.9)	0.2 (2.8)	4.5 (4.8)
Lymphocyte count (×10 ⁹ /L)	1.2 (0.5)	1.7 (0.3)	0.8 (0.4)	1.4 (0.3)	0.7 (0.6)	1.1 (0.6)
Biochemistry						
Potassium (mmol/L)	4.7 (0.4)	5.1 (1.0)	5.2 (0.9)	5.3 (1.0)	4.6 (0.4)	4.8 (0.3)
Creatinine (mmol/L)	0.09 (0.03)	0.09 (0.03)	0.1 (0.07)	0.13 (0.04)	0.09 (0.005)	0.13 (0.05)
Bilirubin (umol/L)	11 (4)	6 (5)	11 (12)	14 (9)	13 (12)	18 (19)
CK (IU/L)	8667 (3889)	8300 (1549)	18,049 (13,363)	19,567 (10,613)	1512 (1317)	10,697 (17,830)
Plasma Cytokines						
IL-6 (pg/ml)	46,531 (17,569)	219,533 (82,887)	40,145 (20,991)	145,060 (54,796)	67,554 (33,134)	64,650 (60,905)
IL-8 (pg/ml)	1171 (934)	490 (235)	2270 (3044)	371 (39)	3135 (1688)	1163 (1479)
IL-10 (pg/ml)	1902 (315)	1889 (499)	2710 (1598)	2093 (752)	2652 (703)	2281 (1580)

Table 1. Characteristics of pulmonary mechanics, hemodynamics and laboratory parameters at 12, 24 and 48 h. All numbers in mean and standard deviation (SD). PEEP, positive end-expiratory pressure; PaCO₂ (mmHg), arterial carbon dioxide partial pressure; CK, creatine kinase; IL, interleukin; OA, oleic acid; OA-LPS, oleic acid and lipopolysaccharides.

damage as compared to OA-LPS. *Sixth*, the amount of lung edema and histological lung injury were comparable among OA and OA-LPS, although there was more necrosis and alveolar hemorrhage in OA, indicating a severe lung damage. There was a trend towards higher levels of plasma cytokines (IL-8 and -10), worse hemodynamic and pulmonary mechanics parameters in OA, indicating that these animals were sicker at 48 h into the study.

OA-LPS animals demonstrated more recruitment potential than OA, while generally displaying more normally aerated lung tissue. These findings are in agreement with the physiological results obtained by blood gas analysis and mechanical ventilation data: driving pressure, dead space ventilation and parameters of oxygenation (PF ratio, oxygenation index) displayed a trend towards improved values in OA-LPS animals as compared to OA. While these results are also partly influenced by other variables (i.e., sicker animals in OA with worse hemodynamic conditions), histopathology evidenced differences between lung injury types. OA animals were shown more tissue necrosis, alveolar hemorrhage and bacterial colonies than OA-LPS, potentially indicating a beneficial effect of corticosteroids in the double-hit model. Corticosteroids express their anti-inflammatory potential through many different signaling pathways⁴², affecting genomic and non-genomic levels in their action. The nuclear factor-kappa B pathway (NF-kB) in particular, one of the known main drivers of local and systemic

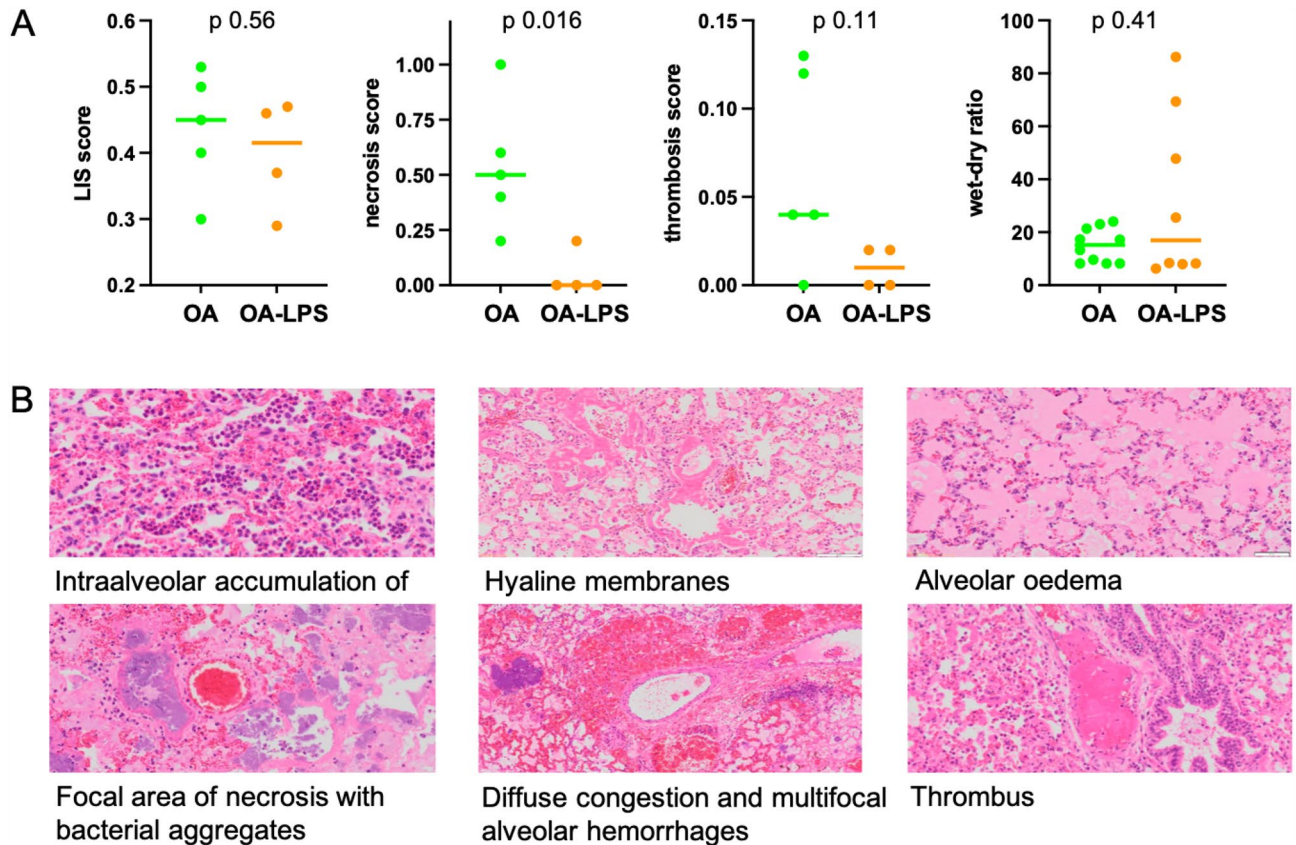


Figure 4. (A) detailed histopathological assessment and (B) representative examples of findings. LIS, lung injury score; OA, oleic acid; OA-LPS, oleic acid and lipopolysaccharides.

inflammation in ARDS^{43,44}, is inhibited by corticosteroids. LPS but not OA activates NF- κ B^{45,46}, offering a partial explanation why treated OA-LPS animals displayed more benefit in terms of pulmonary inflammation and therefore associated recruitable lung tissue. The throughout higher neutrophil count in OA-LPS is likely a direct effect of endotoxin application, it is possible that this reduced the formation of bacterial settlement in the lungs.

OA displayed higher levels of strain. Lung strain represents pulmonary tissue deformation defined as the ratio between tidal volume and End-Expiratory Lung Volume (Vt/EELV)³. A threshold limit in global pulmonary strain has been identified in preventing lung edema and related VILI, thus reducing systemic inflammation and multiorgan dysfunction³. Retamal et al. correlated regional volumetric lung strain with regional inflammation in a 2-hit ARDS model in pigs, evaluating CT and PET imaging simultaneously. The study reported evidence that some lung regions may be exposed to even higher values of regional strain than the global estimated one⁴⁷. Lung edema caused by higher strain led to more non- or poorly aerated tissue. However, our results showed no clear association between a higher amount of pulmonary edema (EVLWI, WD ratio) and strain in both phenotypes.

By applying latent class analysis to parameters of gas exchange, respiratory mechanics and CT-derived lung volumes in 238 patients, Wendel et al.⁴⁸ identified two pulmonary phenotypes: phenotype 1 (non-recruitable) and 2 (recruitable). Phenotype 2 was characterized by more ventilated tissue, higher compliance, and PF ratio after recruitment maneuvers. As inflammatory and laboratory parameters were not recorded, it can only be speculated to what extent these phenotypes overlap with the hyper- and hypoinflammatory subphenotypes as described previously^{17–21}. The lower compliance, more severe acidosis, and higher ICU mortality as seen in the recruitable phenotype match the hyperinflammatory subphenotype as described by Calfee et al., the distribution of required vasopressor dosage, PF ratio, and ICU scores, however, do not match. Although there is no imaging available in the datasets that identified hyper- and hypoinflammatory subphenotype^{17–21}, the response to PEEP as seen in the hyperinflammatory subphenotype¹⁷ indicates at least some overlap with the recruitable phenotype.

Our ovine model of hyperinflammatory ARDS has previously shown a substantial overlap with the human hyperinflammatory subphenotype³¹. We hypothesize that treatment with anti-inflammatory agents, improved inflammatory response, hemodynamic parameters and metabolic condition in ovine OA-LPS, and resulted in more normally aerated and recruitable lung tissue overall as well as less strain. The next step in translation into clinical practice ought to be personalized phenotyping of human ARDS subphenotypes incorporating omics data and imaging techniques to build a thoroughly comprehensive understanding. Urgently needed is (a) an easily applicable biomarker to identify subphenotypes at bedside and (b) imaging data that informs about recruitment potential and regional lung inhomogeneities. This could allow clinicians treatment allocation of specific ARDS subphenotypes and assessment of recruitment potential for application of safer ventilation strategies for improvement of gas exchange without adding VILI.

Important strengths of this study incorporate the use of an established model of ovine ARDS subphenotypes and a controlled setting with allocation concealment and blinding to treatment.

We report several limitations: *First*, as this was a concomitant study, the small number of animals per group available for assessment, results in an exploratory and hypothesis-generating study that will need confirmation in a larger setting. *Second*, as only animals with survival up to 48 h were eligible for CT scan, a selection bias is possible. *Third*, this study did not include imaging of control animals. Therefore, the possible benefit of anti-inflammatory treatment overall cannot be confirmed in scans from untreated ARDS animals. Fourth, although the used CT analysis method has already been validated in establishing aeration compartments of the lung in both human and animal studies, this technique has several intrinsic limitations based on assumptions on voxel analysis⁷. *Fifth*, there is no imaging available at baseline, therefore we can only hypothesize that observed differences are the result of a higher responsiveness to anti-inflammatory treatment rather than a consequence of the used double-hit model. *Sixth*, the shape of the chest wall in sheep is different than in humans with consecutively different elastance properties.

Conclusion

Anti-inflammatory treatment might be beneficial in terms of overall ventilated lung portion and recruitment potential, especially in the OA-LPS group.

Data availability

The dataset generated and analysed during the current study are not publicly available due to being part of a PhD project but are available from the corresponding author on reasonable request.

Received: 29 October 2023; Accepted: 22 January 2024

Published online: 25 January 2024

References

- Ashbaugh, D. G., Bigelow, D. B., Petty, T. L. & Levine, B. E. Acute respiratory distress in adults. *Lancet* **2**, 319–323 (1967).
- Cressoni, M. *et al.* Lung inhomogeneity in patients with acute respiratory distress syndrome. *Am. J. Respir. Crit. Care Med.* **189**, 149–158 (2014).
- Protti, A. *et al.* Lung stress and strain during mechanical ventilation: Any safe threshold?. *Am. J. Respir. Crit. Care Med.* **183**, 1354–1362 (2011).
- Protti, A. *et al.* Lung stress and strain during mechanical ventilation: Any difference between statics and dynamics?. *Crit. Care Med.* **41**, 1046–1055 (2013).
- Adhikari, N. K. J. *et al.* Inhaled nitric oxide does not reduce mortality in patients with acute respiratory distress syndrome regardless of severity. *Crit. Care Med.* **42**, 404–412 (2014).
- Gattinoni, L., Pesenti, A., Avalli, L., Rossi, F. & Bombino, M. Pressure-volume curve of total respiratory system in acute respiratory failure. Computed tomographic scan study. *Am. Rev. Respir. Dis.* **136**, 730–736 (1987).
- Gattinoni, L., Caironi, P., Pelosi, P. & Goodman, L. R. What has computed tomography taught us about the acute respiratory distress syndrome?. *Am. J. Respir. Crit. Care Med.* **164**, 1701–1711 (2001).
- Crotti, S. *et al.* Recruitment and derecruitment during acute respiratory failure: A clinical study. *Am. J. Respir. Crit. Care Med.* **164**, 131–140 (2001).
- Gattinoni, L. *et al.* Lung recruitment in patients with the acute respiratory distress syndrome. *N. Engl. J. Med.* **354**, 1775–1786 (2006).
- Guérin, C. *et al.* Prone positioning in severe acute respiratory distress syndrome. *N. Engl. J. Med.* **368**, 2159–2168 (2013).
- Brower, R. G. *et al.* Ventilation with lower tidal volumes as compared with traditional tidal volumes for acute lung injury and the acute respiratory distress syndrome. *N. Engl. J. Med.* **342**, 1301–1308 (2000).
- Guérin, C. *et al.* Prone position in ARDS patients: Why, when, how and for whom. *Intensive Care Med.* <https://doi.org/10.1007/s00134-020-06306-w> (2020).
- Lamm, W. J., Graham, M. M. & Albert, R. K. Mechanism by which the prone position improves oxygenation in acute lung injury. *Am. J. Respir. Crit. Care Med.* **150**, 184–193 (1994).
- Santini, A. *et al.* Prone position ameliorates lung elastance and increases functional residual capacity independently from lung recruitment. *Intensive Care Med. Exp.* **3**, 1–8 (2015).
- Albert, R. K., Leasa, D., Sanderson, M., Robertson, H. T. & Hlastala, M. P. The prone position improves arterial oxygenation and reduces shunt in oleic-acid-induced acute lung injury. *Am. Rev. Respir. Dis.* **135**, 628–633 (1987).
- Bellani, G. *et al.* Epidemiology, patterns of care, and mortality for patients with acute respiratory distress syndrome in intensive care units in 50 countries. *J. Am. Med. Assoc.* **315**, 788–800 (2016).
- Calfee, C. S. *et al.* Subphenotypes in acute respiratory distress syndrome: Latent class analysis of data from two randomised controlled trials. *Lancet Respir. Med.* **2**, 611–620 (2014).
- Famous, K. R. *et al.* Acute respiratory distress syndrome subphenotypes respond differently to randomized fluid management strategy. *Am. J. Respir. Crit. Care Med.* **195**, 331–338 (2017).
- Bos, L. D. *et al.* Identification and validation of distinct biological phenotypes in patients with acute respiratory distress syndrome by cluster analysis. *Thorax* **72**, 876–883 (2017).
- Calfee, C. S. *et al.* Acute respiratory distress syndrome subphenotypes and differential response to simvastatin: secondary analysis of a randomised controlled trial. *Lancet Respir. Med.* **6**, 691–698 (2018).
- Sinha, P. *et al.* Latent class analysis-derived subphenotypes are generalisable to observational cohorts of acute respiratory distress syndrome: A prospective study. *Thorax* **77**, 13–21 (2022).
- Sinha, P. *et al.* Latent class analysis of ARDS subphenotypes: a secondary analysis of the statins for acutely injured lungs from sepsis (SAILS) study. *Intensive Care Med.* **44**, 1859–1869 (2018).
- Sinha, P. *et al.* Latent class analysis reveals COVID-19-related acute respiratory distress syndrome subgroups with differential responses to corticosteroids. *Am. J. Respir. Crit. Care Med.* **204**, 1274–1285 (2021).
- Chen, H. *et al.* Corticosteroid therapy is associated with improved outcome in critically ill patients with COVID-19 with hyper-inflammatory phenotype. *Chest* **159**, 1793–1802 (2021).
- Prescott, H. C., Calfee, C. S., Taylor Thompson, B., Angus, D. C. & Liu, V. X. Toward smarter lumping and smarter splitting: Rethinking strategies for sepsis and acute respiratory distress syndrome clinical trial design. *Am. J. Respir. Crit. Care Med.* **194**, 147–155 (2016).

26. Ware, L. B., Matthay, M. A. & Mebazaa, A. Designing an ARDS trial for 2020 and beyond: Focus on enrichment strategies. *Intensive Care Med.* <https://doi.org/10.1007/s00134-020-06232-x> (2020).
27. Wick, K. D. *et al.* Promises and challenges of personalized medicine to guide ARDS therapy. *Crit. Care* **25**, 1–15 (2021).
28. Goodman, L. R. *et al.* Adult respiratory distress syndrome due to pulmonary and extrapulmonary causes: CT, clinical, and functional correlations. *Radiology* **213**, 545–552 (1999).
29. Terragni, P. P. *et al.* Tidal hyperinflation during low tidal volume ventilation in acute respiratory distress syndrome. *Am. J. Respir. Crit. Care Med.* **175**, 160–166 (2007).
30. Constantin, J.-M. *et al.* Personalised mechanical ventilation tailored to lung morphology versus low positive end-expiratory pressure for patients with acute respiratory distress syndrome in France (the LIVE study): A multicentre, single-blind, randomised controlled trial. *Lancet Respir. Med.* **7**, 870–880 (2019).
31. Millar, J. E. *et al.* Characterizing preclinical sub-phenotypic models of acute respiratory distress syndrome: An experimental ovine study. *Physiol. Rep.* **9**, e15048 (2021).
32. Wildi, K. *et al.* Validation of messenger ribonucleic acid markers differentiating among human acute respiratory distress syndrome subgroups in an ovine model of acute respiratory distress syndrome phenotypes. *Front. Med.* **9**, 1–7 (2022).
33. Wildi, K. *et al.* Application of anti-inflammatory treatment in two different ovine Acute Respiratory Distress Syndrome injury models: A preclinical randomized intervention study. *Sci. Rep.* **13**, 17986 (2023).
34. Percie du Sert, N. *et al.* Reporting animal research: Explanation and elaboration for the ARRIVE guidelines 2.0. *PLoS Biol.* **18**, e3000411 (2020).
35. Mercat, A. *et al.* Positive end-expiratory pressure setting in adults with acute lung injury and acute respiratory distress syndrome: A randomized controlled trial. *J. Am. Med. Assoc.* **299**, 646–655 (2008).
36. Chiumello, D. *et al.* Assessment of lung aeration and recruitment by CT scan and ultrasound in acute respiratory distress syndrome patients. *Crit. Care Med.* **46**, 1761–1768 (2018).
37. Coppola, S. *et al.* Respiratory mechanics, lung recruitability, and gas exchange in pulmonary and extrapulmonary acute respiratory distress syndrome. *Crit. Care Med.* **47**, 792–799 (2019).
38. Cressoni, M. *et al.* Limits of normality of quantitative thoracic CT analysis. *Crit. Care* **17**, 1–12 (2013).
39. Blankman, P., Hasan, D., Bikker, I. G. & Gommers, D. Lung stress and strain calculations in mechanically ventilated patients in the intensive care unit. *Acta Anaesthesiol. Scand.* **60**, 69–78 (2016).
40. Bouquet, M. *et al.* Development and validation of ELISAs for the quantitation of interleukin (IL)-1 β , IL-6, IL-8 and IL-10 in ovine plasma. *J. Immunol. Methods* **486**, 112835 (2020).
41. Matute-Bello, G. *et al.* An official american thoracic society workshop report: Features and measurements of experimental acute lung injury in animals. *Am. J. Resp. Cell. Mol. Biol.* **44**, 725–738 (2011).
42. Rhen, T. & Cidlowski, J. A. Antiinflammatory action of glucocorticoids—New mechanisms for old drugs. *N. Engl. J. Med.* **353**, 1711–1723 (2005).
43. Meduri, G. U., Muthiah, M. P., Carratu, P., Ertorky, M. & Chrousos, G. P. Nuclear factor- κ B- and glucocorticoid receptor α -mediated mechanisms in the regulation of systemic and pulmonary inflammation during sepsis and acute respiratory distress syndrome: Evidence for inflammation-induced target tissue resistance to glucocorticoids. *Neuroimmunomodulation* **12**, 321–338 (2005).
44. Umberto Meduri, G., Tolley, E. A., Chrousos, G. P. & Stentz, F. Prolonged methylprednisolone treatment suppresses systemic inflammation in patients with unresolving acute respiratory distress syndrome: Evidence for inadequate endogenous glucocorticoid secretion and inflammation-induced immune cell resistance to glucocorticoids. *Am. J. Respir. Crit. Care Med.* **165**, 983–991 (2002).
45. Moine, P. *et al.* NF- κ B regulatory mechanisms in alveolar macrophages from patients with acute respiratory distress syndrome. *Shock* **13**, 85–91 (2000).
46. Chen, H., Bai, C. & Wang, X. The value of the lipopolysaccharide-induced acute lung injury model in respiratory medicine. *Expert Rev. Respir. Med.* **4**, 773–783 (2010).
47. Retamal, J. *et al.* Does regional lung strain correlate with regional inflammation in acute respiratory distress syndrome during nonprotective ventilation? An experimental porcine study. *Crit. Care Med.* **46**, p591-599 (2018).
48. Wendel Garcia, P. D. *et al.* Latent class analysis to predict intensive care outcomes in Acute Respiratory Distress Syndrome: A proposal of two pulmonary phenotypes. *Crit. Care* **25**, 1–11 (2021).

Author contributions

Conception and design of work: K.W., S.M.C., G.L.B., J.F. Acquisition of data: K.W., S.M.C., D.M., C.A., S.H., N.S., K.S., K.L., M.B., E.W., M.P., K.H., S.L., M.D.F., C.P., W.S., J.S., G.L.B., J.F. Analysis and interpretation of data: K.W., S.M.C., M.D.F., J.F. Drafting the work or revising it critically for important intellectual content: K.W., S.M.C., D.M., C.A., S.H., N.S., K.S., K.L., M.B., E.W., M.P., K.H., S.L., M.D.F., C.P., W.S., J.S., G.L.B., J.F. Final approval of the version submitted for publication: K.W., S.M.C., D.M., C.A., S.H., N.S., K.S., K.L., M.B., E.W., M.P., K.H., S.L., M.D.F., C.P., W.S., J.S., G.L.B., J.F. Agreement to be accountable for all aspects of the submitted work: K.W., S.M.C., D.M., C.A., S.H., N.S., K.S., K.L., M.B., E.W., M.P., K.H., S.L., M.D.F., C.P., W.S., J.S., G.L.B., J.F.

Competing interests

This study was funded by the Wesley Medical Research Foundation (2020CR25) and an innovation grant by the Prince Charles Hospital Foundation (INN2018-101) (all KW).

Dr. Karin Wildi has received research funding from the Gottfried und Julia Bangerter-Rhyner Foundation and the University of Basel (both Switzerland). In addition, she received a PhD scholarship from the University of Queensland (Brisbane, Australia). Samantha Livingstone received a PhD scholarship from the Prince Charles Hospital Foundation. Keibun Liu received a research grant from Senko Medical Instrument Mfg. Co., Ltd and the Prince Charles Hospital Foundation. Silver Heinsar received a PhD scholarship from the Prince Charles Hospital Foundation. Kei Sato received a PhD scholarship from the University of Queensland. Jacky Suen received an Advance Queensland Industry Research Fellowship. Gianluigi Li Bassi acknowledges receipt of a “BITRECS” fellowship; the “BITRECS” project has received funding from the European Union’s Horizon 2020 research and innovation program under the Marie Skłodowska-Curie grant agreement no. 754550 and from the “La Caixa” Foundation (ID 100,010,434), under the agreement LCF/PR/GN18/50,310,006. Gianluigi Li Bassi and John Fraser also received research grants from Fisher & Paykel through their affiliated research institution.

Additional information

Supplementary Information The online version contains supplementary material available at <https://doi.org/10.1038/s41598-024-52698-w>.

Correspondence and requests for materials should be addressed to K.W. or G.L.B.

Reprints and permissions information is available at www.nature.com/reprints.

Publisher's note Springer Nature remains neutral with regard to jurisdictional claims in published maps and institutional affiliations.



Open Access This article is licensed under a Creative Commons Attribution 4.0 International License, which permits use, sharing, adaptation, distribution and reproduction in any medium or format, as long as you give appropriate credit to the original author(s) and the source, provide a link to the Creative Commons licence, and indicate if changes were made. The images or other third party material in this article are included in the article's Creative Commons licence, unless indicated otherwise in a credit line to the material. If material is not included in the article's Creative Commons licence and your intended use is not permitted by statutory regulation or exceeds the permitted use, you will need to obtain permission directly from the copyright holder. To view a copy of this licence, visit <http://creativecommons.org/licenses/by/4.0/>.

© The Author(s) 2024